

Published in final edited form as:

Int J Radiat Oncol Biol Phys. 2010 November 15; 78(4): 1193–1200. doi:10.1016/j.ijrobp.2010.05.045.

Effect of hyperoxygenation on tissue pO₂ and its consequence on radiotherapeutic efficacy of orthotopic F98 gliomas

Nadeem Khan, Ph.D^{1,2,*}, Sriram Mupparaju, M.S^{1,2}, Shahryar K. Hekmatyar, Ph.D³, Huagang Hou, M.D^{1,2}, Jean P. Lariviere, B.A^{1,2}, Eugene Demidenko, Ph.D^{1,2}, David J. Gladstone, Sc.D², Risto A. Kauppinen, M.D, Ph.D³, and Harold M. Swartz, M.D, Ph.D^{1,2}

¹EPR Center for Viable Systems, Dartmouth Medical School, Hanover, NH, 03755

²Norris Cotton Cancer Center, Dartmouth-Hitchcock Medical Center, Lebanon, NH 03756

³Biomedical NMR Research Center, Dartmouth Medical School, Hanover, NH 03755

Abstract

Purpose—Lack of methods for repeated assessment of tumor pO₂ limits the ability to test and optimize hypoxia modifying procedures being developed for clinical applications. We report the repeated measurements of orthotopic F98 tumor pO₂, and relate this to the effect of carbogen inhalation on tumor growth when combined with hypofractionated radiotherapy.

Methods and Materials—Electron Paramagnetic Resonance (EPR) oximetry was used for repeated measurements of tumor and contralateral brain pO₂ in rats during 30% O₂ and carbogen inhalation for 5 consecutive days. The T₁ enhanced volumes and diffusion coefficients of the tumors were assessed by MRI. The tumors were irradiated with 9.3 Gy × 4 in rats breathing 30% O₂ or carbogen to determine the effect on tumor growth.

Results—The pre-treatment F98 tumor pO₂ varied between 8 – 16 mmHg, while the contralateral brain had 41 – 45 mmHg pO₂ during repeated measurements. Carbogen breathing led to a significant increase in tumor and contralateral brain pO₂; however this effect declined over days. Irradiation of the tumors in rats breathing carbogen resulted in a significant decrease in tumor growth and an increase in the diffusion coefficient measured by MRI.

Conclusions—The results provide quantitative measurements of the effect of carbogen inhalation on intracerebral tumor pO₂ and its consequence on therapeutic outcome. Such direct repeated pO₂ measurements by EPR oximetry can provide temporal information that could be used to improve therapeutic outcome by scheduling doses at times of improved tumor oxygenation. EPR oximetry is currently being tested for clinical applications.

Keywords

F98 glioma; EPR oximetry; MRI; pO₂; Radiotherapy

© 2010 Elsevier Inc. All rights reserved.

*Address for correspondence and reprint request: Nadeem Khan, Ph.D, EPR Center for Viable Systems, 703 Vail, Dartmouth Medical School, Hanover, NH 03755, USA, Lab: (603) 653-3591; Fax: (603) 650-1717, Nadeem.khan@dartmouth.edu.

Publisher's Disclaimer: This is a PDF file of an unedited manuscript that has been accepted for publication. As a service to our customers we are providing this early version of the manuscript. The manuscript will undergo copyediting, typesetting, and review of the resulting proof before it is published in its final citable form. Please note that during the production process errors may be discovered which could affect the content, and all legal disclaimers that apply to the journal pertain.

Conflict of Interest Notification

No conflict of interest.

Introduction

Malignant gliomas are the most angiogenic tumors with rapid infiltrative growth and profound microvascular proliferation (1,2). The standard treatment protocol is surgical resection followed by chemoradiation and then adjuvant maintenance chemotherapy (3,4). Radiotherapy involves a spectrum of fractionated regimens based on the clinical and anatomical characteristics of the tumor but are rarely based on their molecular or physiological characteristics (5,6). The development of stereotactic techniques have made dose/fraction escalation possible, which has reduced the overall treatment time while preserving local control and sparing normal tissue (7,8). However, despite aggressive multimodality approaches, the prognosis of glioblastoma patients remains poor with a median survival of 14 months and a 2 year survival of less than 30% (3,9). New treatment strategies are urgently needed to improve the therapeutic outcome of these aggressive tumors.

The radioresistance is attributed to several factors including low intrinsic radiosensitivity, high fractions of hypoxic tumor cells, and clonogenic cells with rapid turnover rates (3,9,10). Among these, tumor hypoxia appears to be the most significant therapeutic problem, which results in radioresistance and also contributes to aggressive tumor characteristics (11,12). Unfortunately, tissue pO_2 of the tumors cannot be predicted by tumor type, stage, or size and therefore it must be measured (13,14). Consequently, techniques that can provide direct repeated measurement of tumor pO_2 could have an important role in the optimization of radiotherapy.

With the development of *in vivo* EPR oximetry, it is now possible to assess the tissue pO_2 of orthotopic gliomas during interventions that target hypoxia (15), and thereby make rapid advances in optimizing these approaches and consequently enhance radiotherapeutic outcome. EPR oximetry requires a one time injection of the oxygen sensitive paramagnetic probes such as lithium phthalocyanine (LiPc) using 25 - 23 gauge needles but the rest of the measurement procedure is entirely non-invasive and can be repeated as required (16–18). It is currently being tested in patients with superficial tumors (less than 10 mm from surface) undergoing radio- and/or chemotherapy with the goal to optimize these therapies by scheduling doses at times of optimal tumor oxygenation (16). The development of multi-site EPR oximetry has further expanded its utility by allowing simultaneous tissue pO_2 measurements at multiple sites in the tumor (with a minimal separation of 1 mm) (19).

We report the tissue pO_2 of intracerebral F98 tumors and contralateral brain of rats breathing 30% O_2 and the effect of carbogen inhalation during five days of repeated experiments using EPR oximetry. The tumors were irradiated (9.3 Gy \times 4) at times of increased tumor oxygenation to determine therapeutic outcome. To our knowledge, this is the first report of the tissue pO_2 of intracerebral F98 tumors, the effect of carbogen inhalation on tumor pO_2 , and its consequence on radiotherapeutic outcome.

Materials and Methods

Animal and tumor models

All animal procedures were conducted in strict accordance with the NIH Guide for the Care and Use of Laboratory Animals and were approved by the Institutional Animal Care and Use Committee of Dartmouth Medical School. The F98 glioma exhibits growth, invasive and genomic characteristics similar to human gliomas (20). Fischer rats (200 – 250 g, Charles River Laboratory, MA), which are syngeneic hosts for F98 gliomas were used in this study.

F98 tumor inoculation and implantation of the oximetry probe

The F98 cells were obtained from ATCC (Manassas, VA) and grown in DMEM medium with 10% FBS and 1% penicillin-streptomycin. The procedures for tumor cell inoculation and EPR oximetry were described earlier (15). Briefly, the intracerebral tumors were established by direct injection of 4×10^4 F98 cells in 10 μ l medium at a depth of 3.5 mm from the skull surface, 1.5 and 3.5 mm left lateral from the midline, and 3 mm posterior to the bregma.

One week after cell injection, two aggregates of LiPc crystals (40 – 60 μ g/each) were injected at a depth of 2 mm into the tumor through the same bore holes used earlier for cell injections. One aggregate of LiPc crystals was injected at the same depth in the right hemisphere, 1.5 mm from the midline. These injections created LiPc deposits with a surface area of approximately 0.5 – 1.5 mm² and reported tissue pO₂ of intracerebral F98 tumors and contralateral brain by EPR oximetry.

MRI was done on day 11 (designated as day 0) after cell inoculation to confirm the intracerebral tumor growth, confirm the position of LiPc aggregates, and to determine the volume and diffusion coefficient (D_{av}) of the tumors. The EPR oximetry measurements were started on day 12 (day 1) and MRI was repeated on day 18 (day 7). The experiments were terminated on day 7 after MRI due to the tumor size constraints in accordance with the IACUC guidelines at Dartmouth.

High-Spatial Resolution Multi-Site (HSR-MS) EPR Oximetry

The procedures for *in vivo* EPR oximetry were described earlier (15,16). HSR-MS oximetry method with over modulation uses two spectra that have been acquired with magnetic field gradients, and an analytic relationship between the spectra is used to estimate the line width for each implant (15,19).

For pO₂ measurements, the anesthetized (1.5% isoflurane, 30% FiO₂) animals were positioned between the magnet poles of the 1.2 GHz (L-band) EPR spectrometer. The body temperature was monitored using a rectal probe and maintained at $37 \pm 0.5^\circ\text{C}$ by the use of a warm air blower and warm water pad. The EPR spectra were recorded at 8 mW to avoid power saturation, with scan times varying from 30 – 60 seconds. The spectra were averaged for 8 min each to enhance the signal to noise ratio for precise pO₂ measurements. No significant difference in the pO₂ values obtained from the two LiPc implants in each tumor was observed, therefore, these were pooled to obtain an average tumor pO₂ in this study.

Magnetic Resonance Imaging (MRI)

The changes in tumor volume as assessed from T₁-weighted images acquired after the intraperitoneal injection of 0.2 mmol/kg of gadopentate (Magnevist, Bayer Healthcare) and the traces of the diffusion tensor ($D_{av} = 1/3 \bar{D}$) were assessed using MRI to determine therapeutic outcome. The images were acquired on a 7T horizontal animal magnet with a bore of 20 cm (Magnex Scientific Ltd, U.K) equipped with actively shielded imaging gradients, maximum gradient strength 77 G/cm, clear bore 90 mm (Resonance Research Incorporated Ltd, MA), and interfaced to a Varian Inova Unity console (Varian Inc, CA). A multi-slice spin echo sequence was used to acquire T₁-weighted images for tumor volume determination 10 min after gadopentate injection with the acquisition parameters: TR = 700 ms, TE 8 ms, 20 slices, no slice gap, slice thickness 1 mm, Field of View (FOV) = 30 mm, 128 \times 128, 2 signal averages per phase encoding step. Tumor volumes were calculated by drawing regions of interest on the contrast enhanced tumor regions using Varian in-built BROWSER software.

D_{av} MRI was used to assess treatment response *in vivo* owing to its established ability to highlight cell kill in brain tumors (21,22). The orientation unbiased D_{av} images were collected with the sequence described by Mori and van Zijl (23). The acquisition parameters were as follows: TR = 2500 ms, TE = 55 ms, FOV 30 mm, 128×64 matrix, 6–10 slices, no slice gap, slice thickness 1 mm, b-values 0, 700 and 1100 sec/mm^2 , 2 signal averages per phase encoding step. The D_{av} images were computed by fitting the three different b-value images into a single exponential with a Matlab routine. Tumor margins were determined from T_1 and D_{av} images as $\pm 5\%$ signal change relative to the contralateral brain. Since carbogen alone is not expected to affect tumor growth, D_{av} images were acquired only in groups (i), (iii) and (iv).

Experiment design

The animals were randomly assigned to four groups (i) Control (30% O_2), $n = 8$; (ii) Carbogen (95% $O_2 + 5\% CO_2$), $n = 9$; (iii) 30% $O_2 + 9.3 \text{ Gy} \times 4$, $n = 9$, and (iv) Carbogen + $9.3 \text{ Gy} \times 4$, $n = 8$. Group (i) was designed to investigate the dynamics of intracerebral F98 tumor and contralateral brain (CLB) pO_2 in rats breathing 30% O_2 during repeated measurements for 5 consecutive days. The effect of carbogen inhalation on tissue pO_2 was investigated in group (ii). The tumors were irradiated to determine the effect of 30% O_2 and carbogen inhalation on tumor growth and diffusion coefficients in groups (iii) and (iv).

Control and carbogen protocols

In group (i), the rats were anesthetized using 1.5% isoflurane with 30% FiO_2 and tissue pO_2 was measured for 25 min (baseline pO_2). After a gap of 1 min, the pO_2 measurements were continued for another 25 min. After 25 min of baseline measurements in group (ii), the inhaled 30% oxygen was replaced by carbogen and the pO_2 measurements were continued for nearly 50 min. There was a 1 min gap between the switching of breathing gas from 30% O_2 to carbogen. These experiments were repeated for five consecutive days.

Irradiation protocols

The choice of the 9.3 Gy dose was determined by a calculation based on the linear quadratic formula for cell survival that calculates “standard equivalent dose (SED)” for planning hypofractionated stereotactic radiotherapy (24,25). The dose of $9.3 \text{ Gy} \times 4$ fractions approximates the biological effect of a 70 Gy dose fractionation plan for F98 gliomas. The tumors (left hemisphere) were irradiated using a Varian Linear Accelerator (Clinac 2100C) with a dose rate of 400 monitor units/min (6 MeV electron beam, $6 \text{ cm} \times 6 \text{ cm}$ applicator).

In group (iii), the pO_2 measurements were continued for 25 min after baseline and the rats were then transferred to the radiation facility. The beam was focused on the rats head with a lead shield to irradiate a semi-circle of 19 mm in diameter on the left hemisphere with tumor while sparing the contralateral brain. The rats were returned to the EPR spectrometer for another 16 min of pO_2 measurements.

In group (iv), the changes in tissue pO_2 were followed for approximately 25 min during carbogen breathing after baseline (30% FiO_2) measurements and the tumors were irradiated. After irradiation, the tissue pO_2 was again measured for 16 min to confirm an increase in tumor pO_2 during irradiation in rats breathing carbogen. The time gap between the end of the EPR measurement and start of the irradiation and the resumption of the EPR measurements after the treatment were approximately 8 – 10 min each. These experiments were repeated from days 1 to 4 and only baseline pO_2 was measured on day 5.

Statistical analysis

The two-sided paired t-test was used to avoid animal heterogeneity in comparison of tissue pO₂ between the baseline and carbogen breathing and the chi-square test on the paired differences was applied for multiple time-point comparisons. The rates of tumor growth were estimated using a multivariate regression model on the log scale where each group is represented via a dummy time variable (26). This is a better approach for rate determination than the linear regression analysis, because at day 0 the mean tumor volume of all the animals should be the same. The coefficient at the time variable in each group on the percent scale represents the relative rate of growth with the standard error and corresponding p-values as a part of the regression routine output. All computations were performed using the statistical package S-Plus 8 (Insightful Inc. Seattle). All data are expressed as Mean ± SE; n is the number of animals in each group (only the positive SE bars are shown in figures for visual clarity).

Results

Tissue pO₂ of untreated intracerebral F98 tumor and contralateral brain

The F98 tumors were hypoxic with a baseline tissue pO₂ of 10 – 11 mmHg on day 1 and no significant change was observed during 25 min of repeated measurements in group (i), Figure 1A. A baseline tumor pO₂ of 8 – 10 mmHg was observed on 4 subsequent days and during 25 min of repeated measurements on each day. No significant difference in the tumor pO₂ was observed over days.

A baseline tissue pO₂ of 40 – 44 mmHg was observed in the CLB on day 1 with no significant change during 25 min of repeated measurement, Figure 1B. The baseline CLB pO₂ varied between 35 – 44 mmHg on subsequent days but was not significantly different from that observed on day 1. Similar results were obtained during 25 min of repeated measurements on each day. The F98 tumors were significantly hypoxic as compared to the CLB during 5 days of repeated measurements.

Effect of carbogen inhalation on intracerebral F98 tumor and contralateral brain pO₂

The effects of carbogen inhalation on the tumor and CLB pO₂ are summarized in Figure 2. A significant increase in the tissue pO₂ of both, tumors and CLB, occurred within 16 min of carbogen inhalation and a maximum increase in the tissue pO₂ was observed at approximately 30 min of carbogen inhalation, Figure 2. Similar results were obtained on days 2 – 5. However, the baseline tumor pO₂ and the magnitude of the increase in pO₂ during carbogen inhalation were significantly smaller than that of the CLB.

Effect of hypofractionated radiotherapy (9.3 Gy × 4) during inhalation of 30% O₂ or carbogen

No significant change in the baseline tumor and CLB pO₂ was observed during 5 days of repeated measurements, Figures 3 and 4. Based on the results of the carbogen experiment (group ii); the tumors were irradiated at the time of a maximal increase in tumor pO₂ i.e. at approximately 35 min of carbogen breathing on days 1 – 4, Figure 3. The tumor pO₂ remained at a significantly higher level before and immediately after radiotherapy. The tumors in rats breathing 30% O₂ were also irradiated at the same time points, Figure 4. The tissue pO₂ of the tumor and CLB observed before and after radiotherapy were not significantly different from the baseline on each day.

Change in the mean baseline tumor and CLB pO₂ and response to carbogen over days

The mean baseline tumor and CLB pO₂ were similar in groups (ii) and (iv) on day 1, Figure 5. However, a significant decrease in the mean baseline tumor (slope, $p = 0.003$) and CLB (slope, $p = 0.0003$) pO₂ occurred over days in group (ii), Figure 5A. Also, their response to the carbogen (slope $p_{\text{tumor}} = 0.005$; slope $p_{\text{CLB}} = 0.0024$) declined significantly over days, Figure 5B. On the other hand, no such changes were observed in group (iv) with the tumors irradiated during carbogen inhalation.

Effect of hyperoxygenation on radiotherapeutic outcome

The tumor volumes and the rate of growth were compared to determine the therapeutic outcome, Table 1. A similar tumor volume was observed on day 0 among groups. The tumor volume, increased significantly on day 7 in each group. The rates of tumor growth were similar in groups (i) and (ii) and no significant changes were observed in group (iii). However, a significant decrease in rate of tumor growth was observed in group (iv) as compared to other groups.

The changes in the mean tumor D_{av} and the histograms are shown in Figures 6 and 7 respectively. The typical images used to determine the diffusion coefficients are shown in Figure 8. No significant difference in the D_{av} between day 0 and day 7 was evident in group (i). A significant decrease in the D_{av} on day 0 was observed in group (iii) as compared to group (i). In contrast, a significant increase in the D_{av} occurred on day 7 in groups (iii) and (iv) as well as an increase in the number of pixels with elevated D_{av} within the tumor.

Discussion

The measurement of pO₂ in gliomas is particularly challenging due to lack of appropriate techniques for repeated measurements in the brain. This was achieved by using state-of-the-art HSR-MS EPR oximetry. The results indicate moderate hypoxia in F98 tumors while the CLB were well oxygenated. Carbogen inhalation resulted in a significant increase in tumor and CLB pO₂ within 16 min, however, the baseline pO₂ and its response to carbogen declined over days. This is likely due to an increase in intracranial pressure and compromised tumor vasculature with tumor growth over days (15). The effect of the carbogen breathing on the dynamics of tumor pO₂ has varied with the tumor type, animal model, and the site of tumor growth (27–29). Using Oxylite, Bussink et al. have reported the effect of carbogen breathing with/without nicotinamide on the tissue pO₂ of subcutaneous human glioblastoma xenograft tumors (E106, E102) and a squamous cell carcinoma of the larynx (SCCNij3) (27). A maximum increase in the tumor pO₂ was observed between 0.8 – 14 min, 0.7 – 16 min and 3 – 16 min in E102, E106 and SCCNij3 tumors respectively. Using a similar oximetry approach, Gu et al. reported a significant increase in the tissue pO₂ of sc mammary adenocarcinoma tumor within 8 min of carbogen breathing which gradually increased over the next 12 min (28). A slow increase in the tissue pO₂ of the subcutaneous rat DS-sarcomas over 15 min during carbogen challenge is reported by Thews et al. (29). Our results, which are consistent with our previous report on the intracerebral 9L and C6 tumors (15), confirm that the oxygenation of the intracerebral tumors appears to take a longer time. This is likely due to the known differences in the responses of the cerebral vasculature to other stimuli, and the different permeability of the cerebral vasculature resulting in the “blood-brain barrier”.

The radiosensitizing effects of carbogen breathing during radiotherapy have also been investigated in various pre-clinical and clinical studies (30). We did not see an increase in F98 tumor pO₂ after radiotherapy. This is in concurrence with our earlier observation with hypoxic intracerebral C6 tumors (15). On the contrary, an increase in tumor pO₂ was

observed when relatively well oxygenated 9L tumors were irradiated by a single dose of 9.3 Gy (15). These results indicate a tumor specific effect of radiotherapy on intracerebral tumor oxygenation as compared to the tumors grown subcutaneously in mice (31,32). The growth rates of the tumors irradiated in rats breathing 30% O₂ were similar to that of the controls. This is consistent with the highly aggressive and radioresistant nature of the F98 tumors (20); characteristics similar to clinical high-grade gliomas. Aggressive therapeutic approaches, such as boron neutron capture therapy (33), synchrotron stereotactic radiotherapy with direct intratumoral injection of cisplatin (34) and photon irradiation with intracerebral delivery of carboplatin using osmotic pumps (35) have shown some survival benefits in rats bearing F98 tumors.

Irradiation of the tumors at the time of an increase in tumor pO₂ during carbogen inhalation resulted in a significant decrease in the rate of tumor growth (~ 50%) as compared to other groups. Interestingly, there was no change in the baseline tissue pO₂ or response to carbogen over days in this group. We speculate that a significant delay in the tumor growth in these experiments did not influence the intracranial pressure and/or tumor vasculature. The increase in D_{av} of the irradiated tumors on day 7 in the carbogen group is an indication of reduced tumor cell density due to the treatment (21,36), which is in agreement with a significant decline in the tumor growth rate observed in this group. These results indicate that the elevated tumor pO₂ during carbogen inhalation renders F98 gliomas more sensitive to irradiation, resulting in cell eradication and tumor shrinkage. However, we failed to detect any significant changes in the growth rate of the tumors in rats breathing 30% O₂ with a similar increase in tumor D_{av}.

In conclusion, orthotopic F98 tumors are hypoxic and their response to carbogen inhalation varied over days. The results emphasize the importance of tumor pO₂ measurements during hypoxia modifying procedures. *In vivo* EPR oximetry has the potential to provide repeated non-invasive tissue pO₂ of orthotopic tumors and could be used to investigate and optimize hypoxia modifying procedures for clinical applications.

Abbreviations

EPR	Electron Paramagnetic Resonance
MRI	Magnetic Resonance Imaging
pO₂	Partial pressure of oxygen
FiO₂	Fraction of inspired oxygen
LiPc	Lithium phthalocyanine
CLB	Contralateral brain
FOV	Field of view

Acknowledgments

NIH grants CA120919 and CA118069 to NK and PO1EB2180 to HMS. The authors thank Harriet St. Laurent and Kerry A. Tillson for assistance in the use of the radiation facility at DHMC.

References

1. Buckner JC, Brown PD, O'Neill BP, et al. Central nervous system tumors. *Mayo Clin Proc.* 2007; 82:1271–1286. [PubMed: 17908533]
2. Kanu OO, Hughes B, Di C, et al. Glioblastoma Multiforme Oncogenomics and Signaling Pathways. *Clin Med Oncol.* 2009; 3:39–52. [PubMed: 19777070]

3. Clarke J, Butowski N, Chang S. Recent advances in therapy for glioblastoma. *Arch Neurol*. 2010; 67:279–283. [PubMed: 20212224]
4. Quick A, Patel D, Hadziahmetovic M, et al. Current therapeutic paradigms in glioblastoma. *Rev Recent Clin Trials*. 2009; 5:14–27. [PubMed: 20205684]
5. Combs SE. Radiation therapy. *Recent Results Cancer Res*. 2009; 171:125–140. [PubMed: 19322541]
6. Romanelli P, Conti A, Pontoriero A, et al. Role of stereotactic radiosurgery and fractionated stereotactic radiotherapy for the treatment of recurrent glioblastoma multiforme. *Neurosurg Focus*. 2009; 27:E1–E11.
7. Nieder C, Astner ST, Mehta MP, et al. Improvement, clinical course, and quality of life after palliative radiotherapy for recurrent glioblastoma. *Am J Clin Oncol*. 2008; 31:300–305. [PubMed: 18525311]
8. Khuntia D, Tome WA, Mehta MP. Radiation techniques in neuro-oncology. *Neurotherapeutics*. 2009; 6:487–499. [PubMed: 19560739]
9. Quick A, Patel D, Hadziahmetovic M, et al. Current Therapeutic Paradigms in Glioblastoma. *Rev Recent Clin Trials*.
10. Preusser M, Haberler C, Hainfellner JA. Malignant glioma: neuropathology and neurobiology. *Wien Med Wochenschr*. 2006; 156:332–337. [PubMed: 16944363]
11. Jensen RL. Brain tumor hypoxia: tumorigenesis, angiogenesis, imaging, pseudoprogression, and as a therapeutic target. *J Neurooncol*. 2009; 92:317–335. [PubMed: 19357959]
12. Oliver L, Olivier C, Marhuenda FB, et al. Hypoxia and the malignant glioma microenvironment: regulation and implications for therapy. *Curr Mol Pharmacol*. 2009; 2:263–284. [PubMed: 20021464]
13. Tatum JL, Kelloff GJ, Gillies RJ, et al. Hypoxia: importance in tumor biology, noninvasive measurement by imaging, and value of its measurement in the management of cancer therapy. *Int J Radiat Biol*. 2006; 82:699–757. [PubMed: 17118889]
14. Vaupel P. Hypoxia and aggressive tumor phenotype: implications for therapy and prognosis. *Oncologist*. 2008; 13(Suppl 3):21–26. [PubMed: 18458121]
15. Khan N, Li H, Hou H, et al. Tissue pO₂ of orthotopic 9L and C6 gliomas and tumor-specific response to radiotherapy and hyperoxygenation. *Int J Radiat Oncol Biol Phys*. 2009; 73:878–885. [PubMed: 19136221]
16. Khan N, Williams BB, Hou H, et al. Repetitive tissue pO₂ measurements by electron paramagnetic resonance oximetry: current status and future potential for experimental and clinical studies. *Antioxid Redox Signal*. 2007; 9:1169–1182. [PubMed: 17536960]
17. Liu KJ, Gast P, Moussavi M, et al. Lithium phthalocyanine: a probe for electron paramagnetic resonance oximetry in viable biological systems. *Proc Natl Acad Sci U S A*. 1993; 90:5438–5442. [PubMed: 8390665]
18. Swartz HM, Clarkson RB. The measurement of oxygen in vivo using EPR techniques. *Phys Med Biol*. 1998; 43:1957–1975. [PubMed: 9703059]
19. Williams BB, Hou H, Grinberg OY, et al. High spatial resolution multisite EPR oximetry of transient focal cerebral ischemia in the rat. *Antioxid Redox Signal*. 2007; 9:1691–1698. [PubMed: 17678442]
20. Barth RF, Kaur B. Rat brain tumor models in experimental neuro-oncology: the C6, 9L, T9, RG2, F98, BT4C, RT-2 and CNS-1 gliomas. *J Neurooncol*. 2009
21. Chenevert TL, McKeever PE, Ross BD. Monitoring early response of experimental brain tumors to therapy using diffusion magnetic resonance imaging. *Clin Cancer Res*. 1997; 3:1457–1466. [PubMed: 9815831]
22. Kauppinen RA. Monitoring cytotoxic tumour treatment response by diffusion magnetic resonance imaging and proton spectroscopy. *NMR Biomed*. 2002; 15:6–17. [PubMed: 11840548]
23. Mori S, van Zijl PC. Diffusion weighting by the trace of the diffusion tensor within a single scan. *Magn Reson Med*. 1995; 33:41–52. [PubMed: 7891534]
24. Denekamp J, Waites T, Fowler JF. Predicting realistic RBE values for clinically relevant radiotherapy schedules. *Int J Radiat Biol*. 1997; 71:681–694. [PubMed: 9246183]

25. Dale RG, Jones B, Sinclair JA. Dose equivalents of tumour repopulation during radiotherapy: the potential for confusion. *Br J Radiol.* 2000; 73:892–894. [PubMed: 11026867]
26. Draper, N.; Smith, H. *Applied Regression Analysis.* 3rd ed.. New York: Wiley; 1998.
27. Bussink J, Kaanders JH, Strik AM, et al. Effects of nicotinamide and carbogen on oxygenation in human tumor xenografts measured with luminescence based fiber-optic probes. *Radiother Oncol.* 2000; 57:21–30. [PubMed: 11033185]
28. Gu Y, Bourke VA, Kim JG, et al. Dynamic response of breast tumor oxygenation to hyperoxic respiratory challenge monitored with three oxygen-sensitive parameters. *Appl Opt.* 2003; 42:2960–2967. [PubMed: 12790445]
29. Thews O, Kelleher DK, Vaupel P. Dynamics of tumor oxygenation and red blood cell flux in response to inspiratory hyperoxia combined with different levels of inspiratory hypercapnia. *Radiother Oncol.* 2002; 62:77–85. [PubMed: 11830315]
30. Bache M, Kappler M, Said HM, et al. Detection and specific targeting of hypoxic regions within solid tumors: current preclinical and clinical strategies. *Curr Med Chem.* 2008; 15:322–338. [PubMed: 18288988]
31. Hou H, Lariviere JP, Demidenko E, et al. Repeated tumor pO₂ measurements by multi-site EPR oximetry as a prognostic marker for enhanced therapeutic efficacy of fractionated radiotherapy. *Radiother Oncol.* 2009; 91(1):126–131. [PubMed: 19013657]
32. Crockart N, Jordan BF, Baudelet C, et al. Early reoxygenation in tumors after irradiation: determining factors and consequences for radiotherapy regimens using daily multiple fractions. *Int J Radiat Oncol Biol Phys.* 2005; 63:901–910. [PubMed: 16199320]
33. Barth RF, Yang W, Rotaru JH, et al. Boron neutron capture therapy of brain tumors: enhanced survival and cure following blood-brain barrier disruption and intracarotid injection of sodium borocaptate and boronophenylalanine. *Int J Radiat Oncol Biol Phys.* 2000; 47:209–218. [PubMed: 10758326]
34. Biston MC, Joubert A, Adam JF, et al. Cure of Fisher rats bearing radioresistant F98 glioma treated with cis-platinum and irradiated with monochromatic synchrotron X-rays. *Cancer Res.* 2004; 64:2317–2323. [PubMed: 15059878]
35. Rousseau J, Barth RF, Moeschberger ML, et al. Efficacy of intracerebral delivery of Carboplatin in combination with photon irradiation for treatment of F98 glioma-bearing rats. *Int J Radiat Oncol Biol Phys.* 2009; 73:530–536. [PubMed: 19147017]
36. Valonen PK, Lehtimaki KK, Vaisanen TH, et al. Water diffusion in a rat glioma during ganciclovir-thymidine kinase gene therapy-induced programmed cell death in vivo: correlation with cell density. *J Magn Reson Imaging.* 2004; 19:389–396. [PubMed: 15065161]

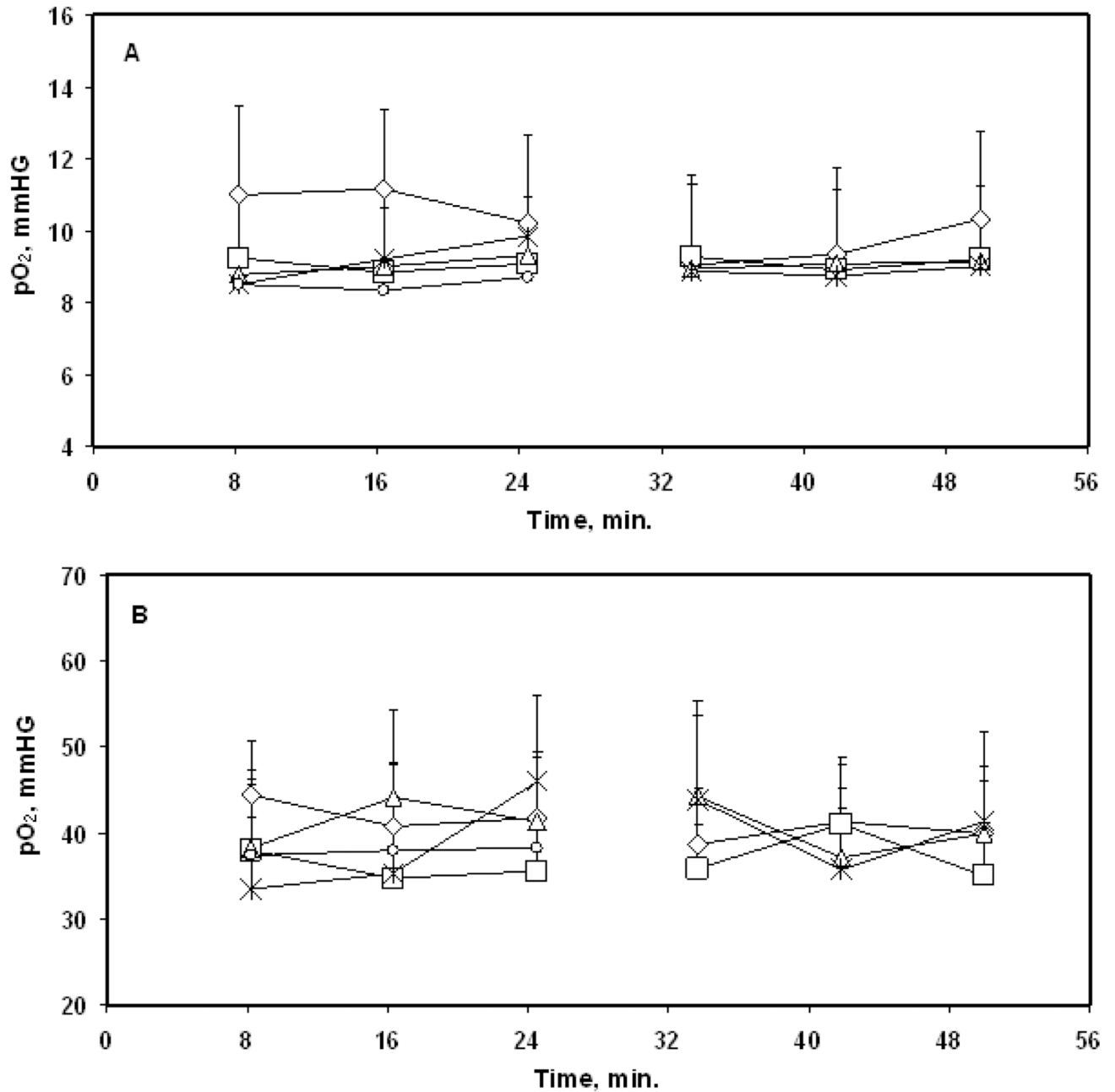


Figure 1.

Tissue pO_2 of (A) intracerebral F98 tumors and (B) contralateral brain of rats breathing 30% O_2 . The tissue pO_2 were measured for 50 min each and the measurements were repeated for five consecutive days. ◇, day 1; □, day 2; △, day 3; *, day 4; ○, day 5. Mean + SE, n = 8.

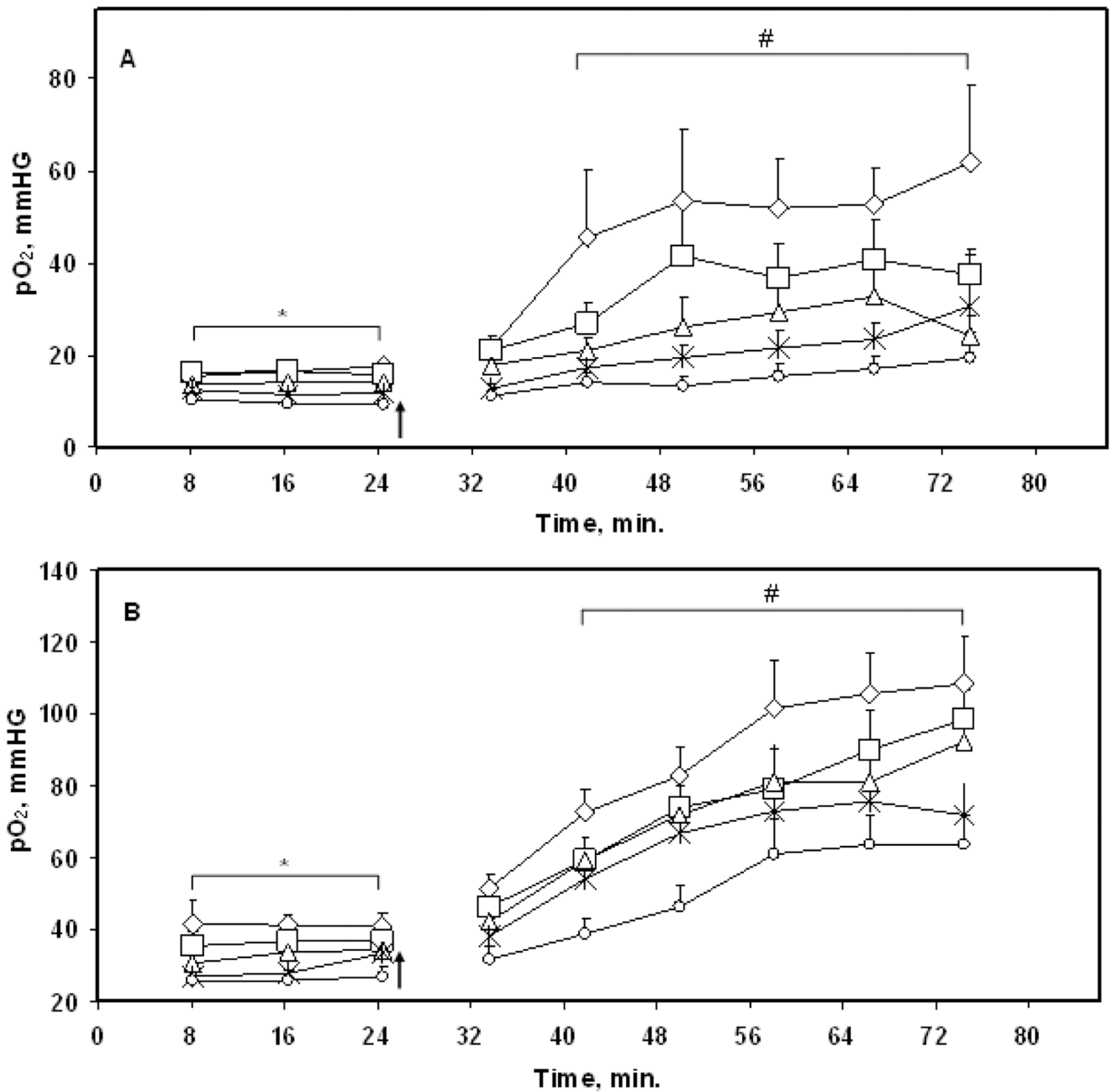


Figure 2.

Tissue pO_2 of (A) intracerebral F98 tumors and (B) contralateral brain of rats during 25 min of 30% O_2 and 50 min of carbogen (5% CO_2 + 95% O_2) inhalation for five consecutive days. ◇, day 1; □, day 2; △, day 3; *, day 4; ○, day 5. The arrow indicates the time at which 30% O_2 was switched to carbogen. * $p < 0.05$, day 1 compared with day 3 – day 5; # $p < 0.05$ compared with baseline on each day, Mean + SE, $n = 9$.

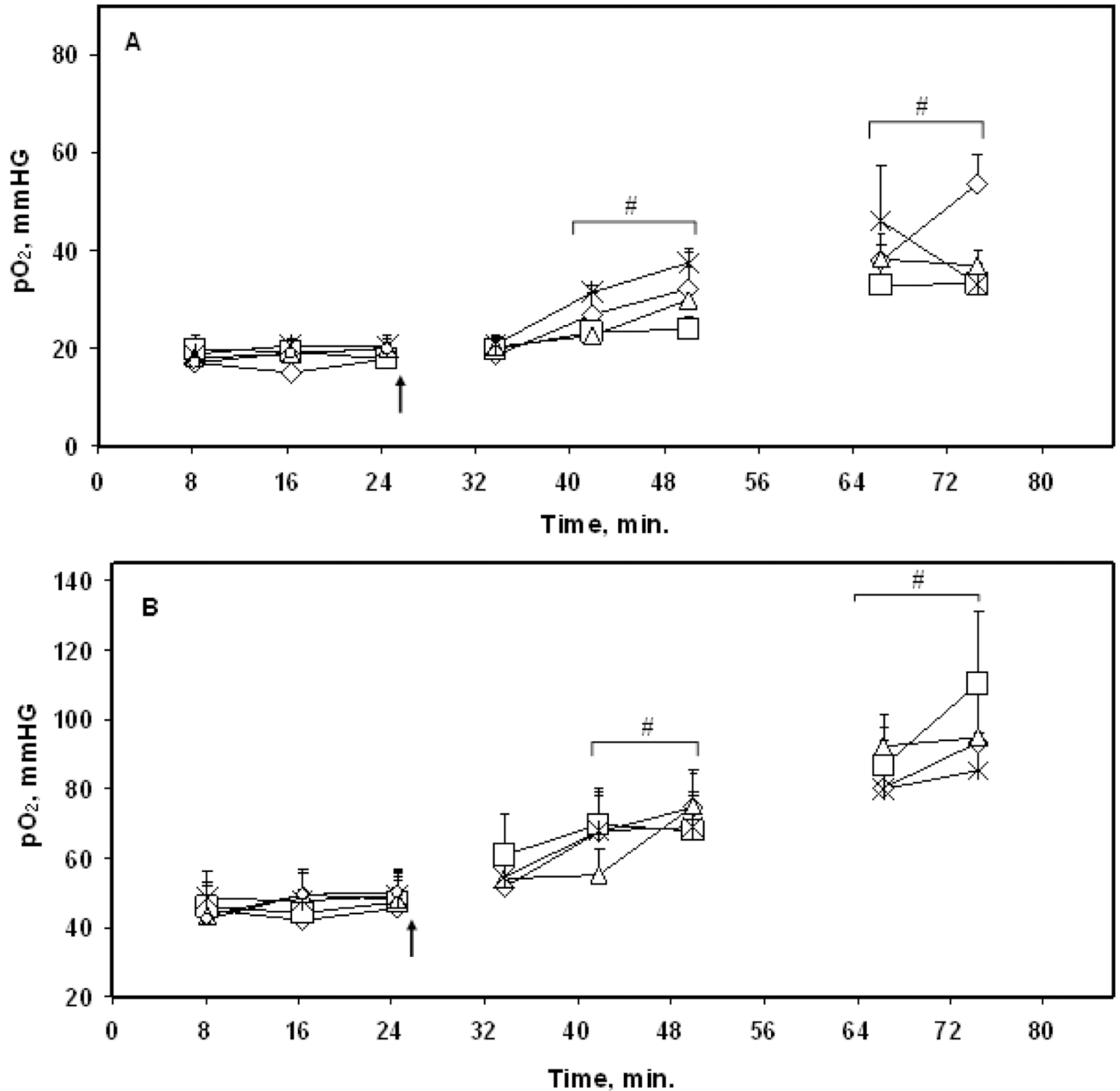


Figure 3.

Tissue pO₂ of (A) intracerebral F98 tumor and (B) contralateral brain in rats during 30% O₂ and carbogen breathing. The tumors were irradiated with 9.3 Gy on day 1 – day 4 at approximately 35 min of carbogen inhalation. The arrow indicates the time when the inhaled gas of 30% O₂ was switched to carbogen. Only a baseline pO₂ was measured on day 5 in rats breathing 30% O₂. ◇, day 1; □, day 2; △, day 3; *, day 4; ○, day 5. # p < 0.05 compared with baseline on each day. Mean + SE, n = 8.

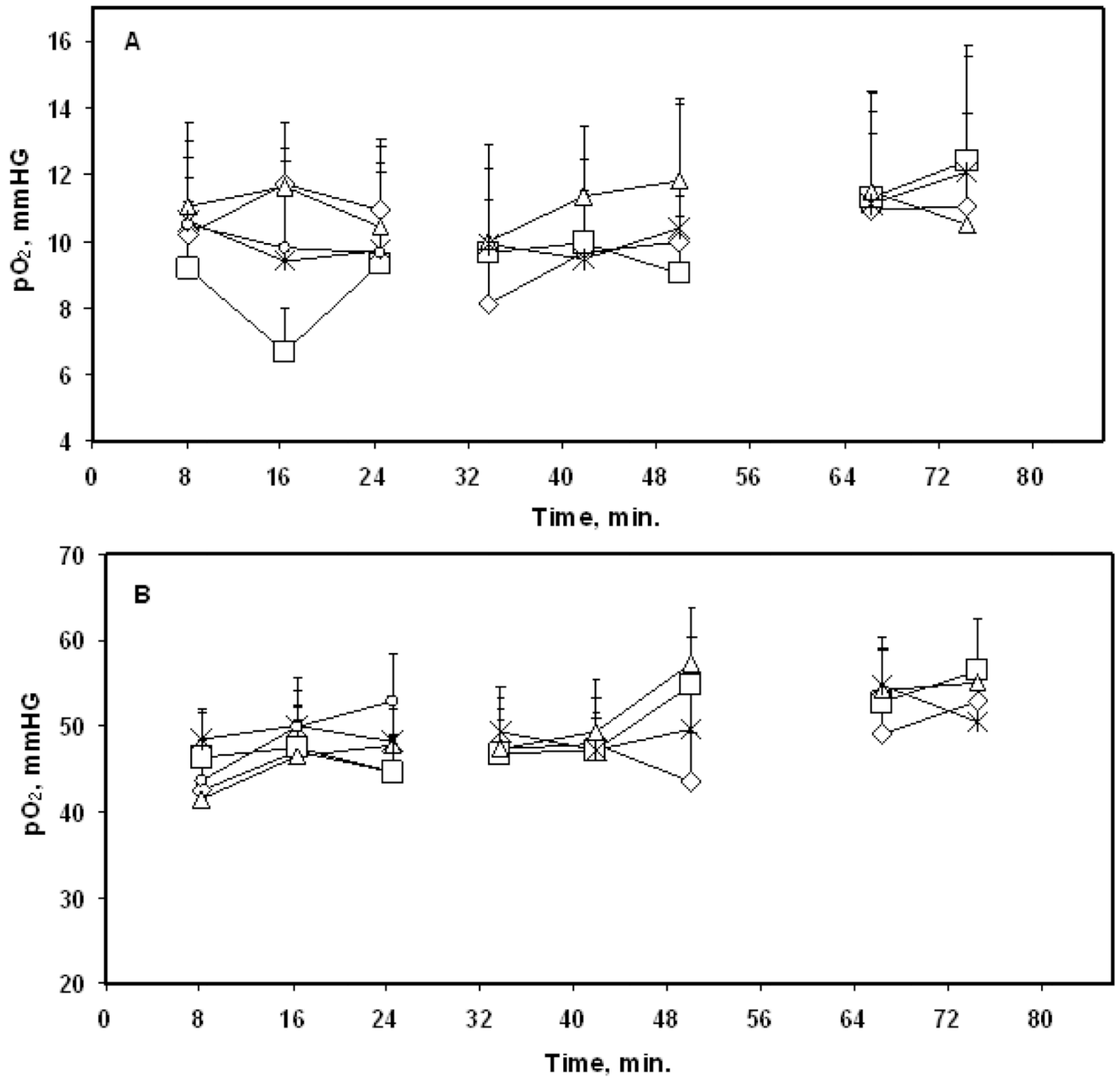


Figure 4. Tissue pO₂ of (A) intracerebral F98 tumor and (B) contralateral brain of rats during 30% O₂ breathing. The tumors were irradiated with 9.3 Gy at approximately 35 min of 30% O₂ breathing after baseline measurements on day 1 – day 4. Only a baseline pO₂ was measured on day 5 in rats breathing 30% O₂. ◇, day 1; □, day 2; △, day 3; *, day 4; ○, day 5. Mean + SE, n = 9.

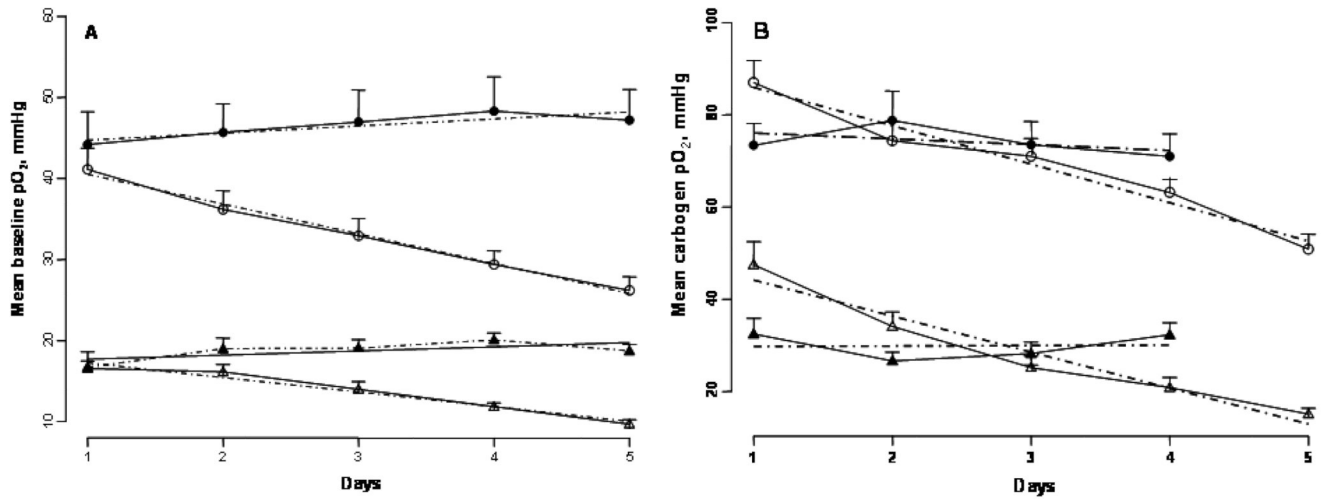


Figure 5.

Mean tissue pO₂ observed during (A) baseline (25 min) and (B) carbogen (50 min) inhalation of intracerebral F98 tumors and contralateral brain in the carbogen alone (Δ: tumor; ○: CLB) and carbogen + 9.3 Gy × 4 (▲: tumor; ●: CLB) groups. The dashed lines indicate the slope of pO₂ change over days. Mean + SE, n = 8 - 9.

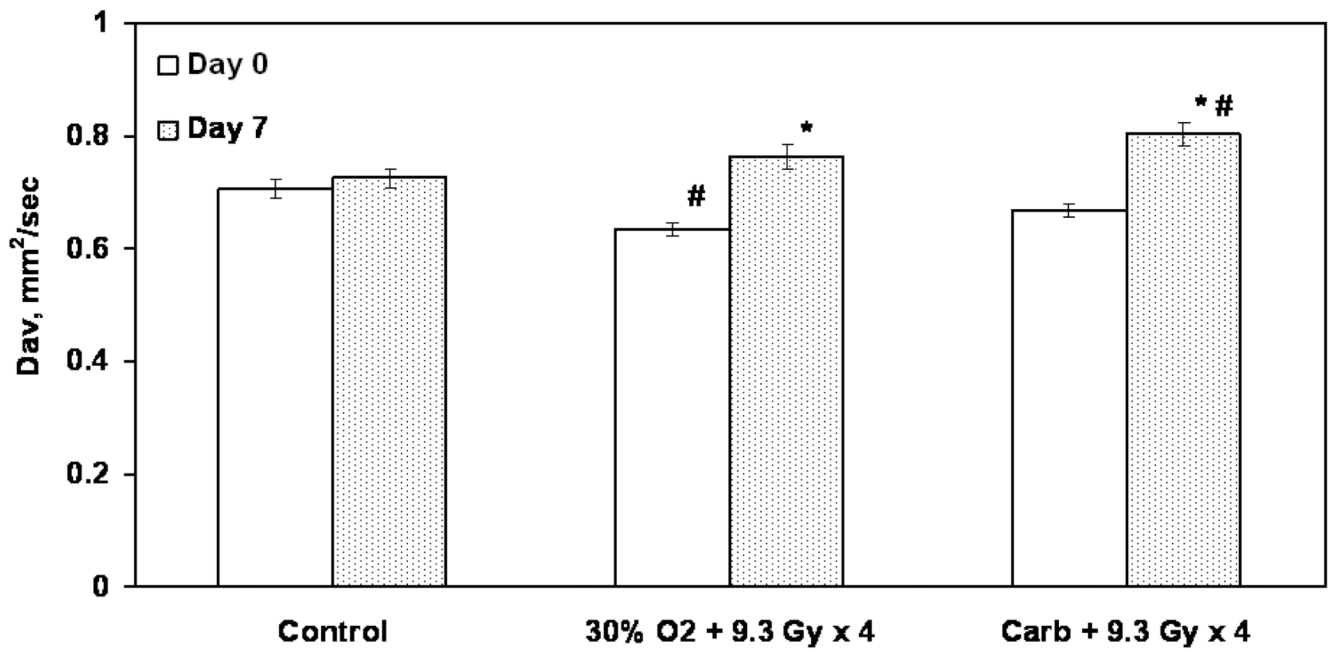


Figure 6.

Trace of the diffusion tensor (D_{av}) of intracerebral F98 tumors on day 0 and day 7 assessed using MRI. * $p < 0.05$ compared with day 0 of each group; # $p < 0.05$ compared with the control. Mean \pm SE, $n = 5 - 6$.

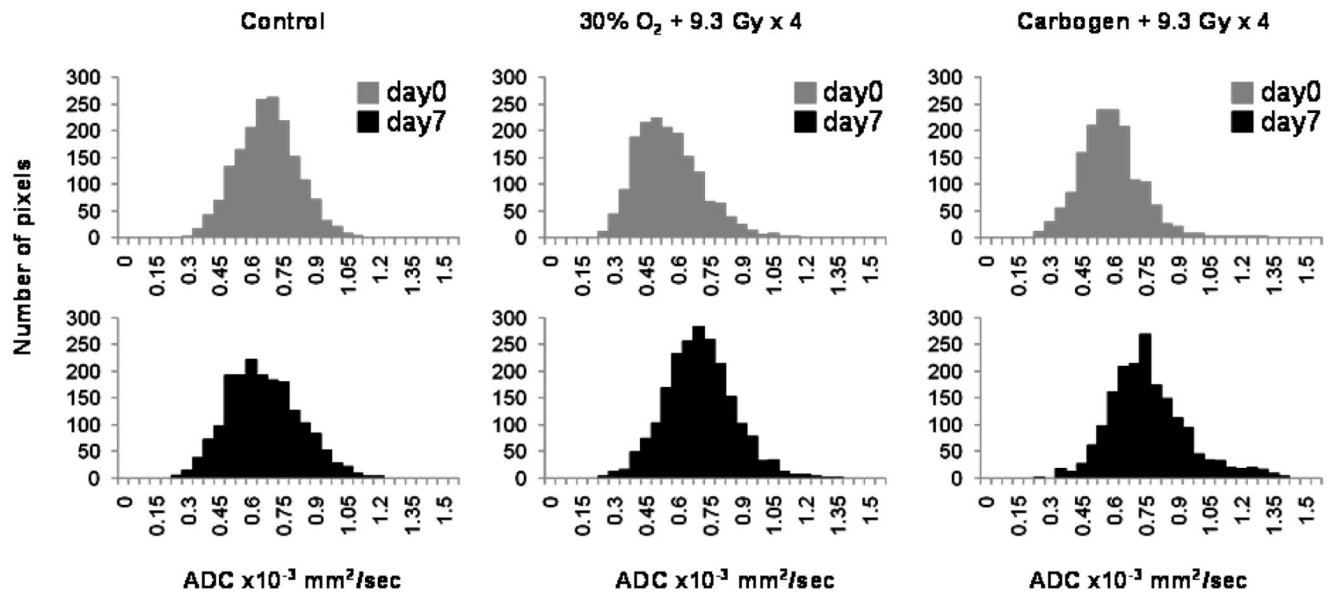


Figure 7.

The D_{av} histograms of the intracerebral F98 tumors on day 0 and day 7 in the control, 30% O₂ + 9.3 Gy × 4 and carbogen + 9.3 Gy × 4 groups. n = 5 – 6.

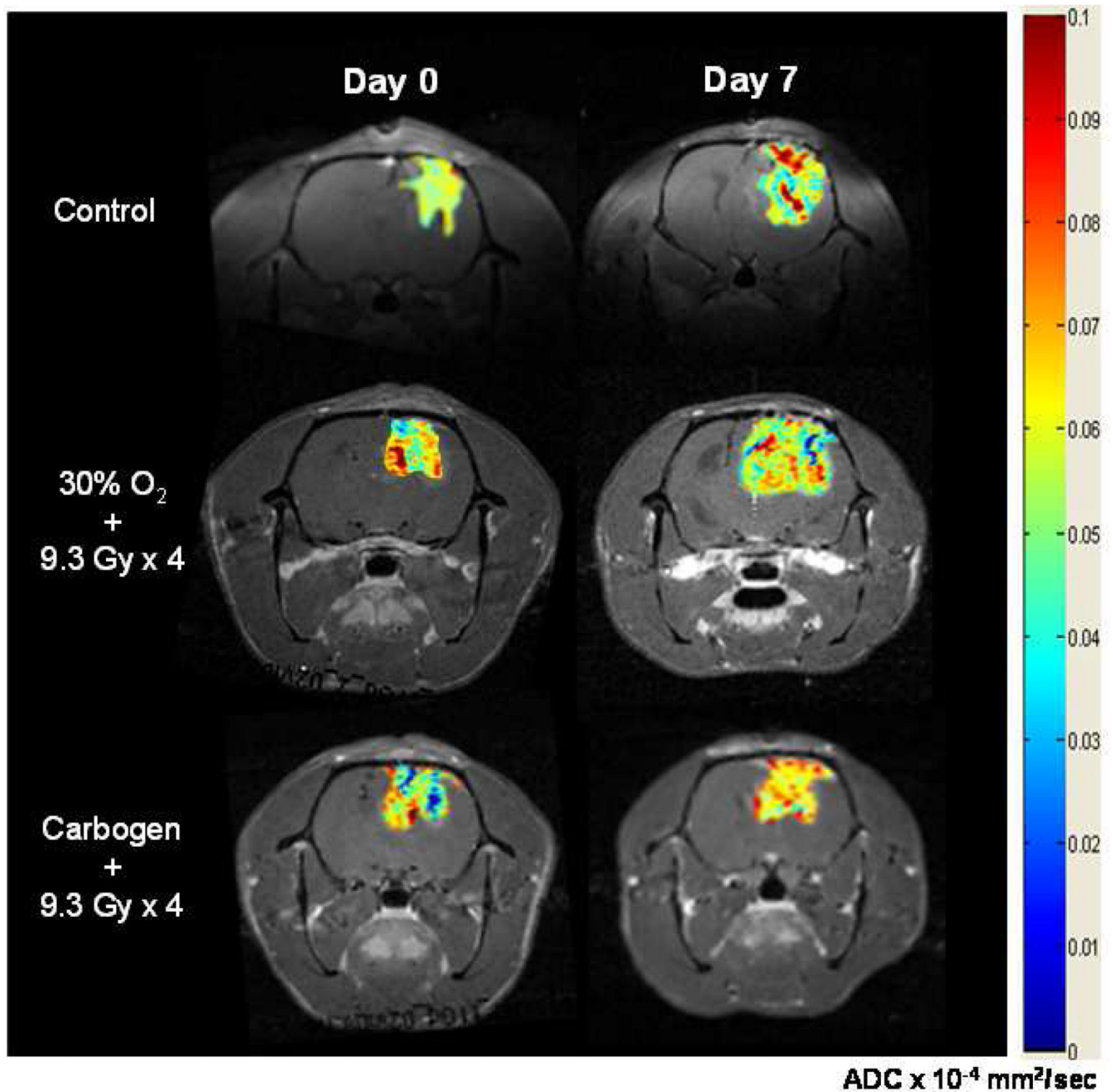


Figure 8.

Typical diffusion images used to assess D_{av} of the intracerebral F98 tumors on day 0 and day 7 in the control, 30% O₂ + 9.3 Gy × 4 and carbogen + 9.3 Gy × 4 groups by MRI. These images were collected with the sequence described by Mori and van Zijl (23).

Table 1

The tumor volume of the intracerebral F98 tumors and rate of growth per day in the control, carbogen alone and irradiation groups.

Group #	Groups	Tumor volume (mm ³ , mean ± SE)		Rate of tumor growth per day (% , mean ± SE)
		Day 0	Day 7	
i	Control (30% O ₂)	103.2 ± 15	226.6 ± 21 *	11.8 ± 1.9
ii	Carbogen alone	94.1 ± 10	250.1 ± 31 *	12.9 ± 2
iii	30% O ₂ + 9.3 Gy × 4	107.5 ± 13	236.5 ± 27 *	12.3 ± 2
iv	Carbogen + 9.3 Gy × 4	104.6 ± 9	156.4 ± 15 *	6.4 ± 1.8 #

The tumor volumes were determined using contrast enhanced MRI.

* p < 0.05 compared with day 0;

p < 0.05 compared with control, carbogen alone and 30% O₂ + 9.3 Gy × 4 groups.